Proc. Natl. Acad. Sci. USA
Vol. 82, pp. 240–244, January 1985
Neurobiology

Functional reconstitution of the purified brain sodium channel in planar lipid bilayers

(excitable membranes/single channels/batrachotoxin/tetrodotoxin/ion selectivity)

ROBERT P. HARTSHORNE*, BERNHARD U. KELLER*, JANE A. TALVENHEIMO†, WILLIAM A. CATTERALL†, AND MAURICIO MONTAL*‡

*Departments of Biology and Physics, University of California at San Diego, La Jolla, CA 92093; and †Department of Pharmacology, University of Washington, Seattle, WA 98195

Communicated by Lubert Stryer, August 31, 1984

ABSTRACT **The ion conduction and voltage dependence of sodium channels purified from rat brain were investigated in planar lipid bilayers in the presence of batrachotoxin. Single channel currents are clearly resolved. Channel opening is voltage dependent and favored by depolarization. The voltage at which the channel is open 50% of the time is −91 ± 17 mV (SD, n = 22) and the apparent gating charge is ≈4. Tetrodotoxin reversibly blocks the ionic current through the sodium channels. The K_i for the tetrodotoxin block is 8.3 nM at −50 mV and is voltage dependent with the K_i increasing e-fold for depolarizations of 43 mV. The single channel conductance, γ, is ohmic. At 0.5 M salt concentrations γ = 25 pS for Na^+, 3.5 pS for K^+, and 1.2 pS for Rb^+. This study demonstrates that the purified brain sodium channel—which consists of three polypeptide subunits: α ($M_r \approx 260{,}000$), $\beta 1$ ($M_r \approx 39{,}000$), and $\beta 2$ ($M_r \approx 37{,}000$)—exhibits the same voltage dependence, neurotoxin sensitivity, and ionic selectivity associated with native sodium channels.**

The sodium channel controls the voltage-dependent changes in sodium conductance that occur during an action potential in electrically excitable tissues. Over the past three decades, sodium channel function was extensively characterized through the use of sophisticated electrophysiological techniques (reviewed in ref. 1). More recently, biochemical techniques were applied to identify the sodium channel protein and to purify it in a detergent-soluble form from eel electroplax (2, 3) rat brain (4, 5), and rat muscle (6, 7). The purified sodium channel protein from all three sources was reconstituted into phospholipid vesicles and shown to retain functional activity by measurements of neurotoxin-mediated $^{22}Na^+$ flux (8–11). The neurotoxins veratridine and batrachotoxin (BTX) are specific sodium channel activators that shift the voltage dependence of activation in the hyperpolarized direction and eliminate inactivation (12–14). Saxitoxin (STX) and tetrodotoxin (TTX) are specific sodium channel blockers that bind to a receptor site on the extracellular-facing side of the sodium channel and inhibit ion translocation (14, 15).

Neurotoxin-mediated sodium flux measurements in reconstituted vesicles played a crucial role in demonstrating the functional integrity of purified sodium channels. This assay, however, lacks the time resolution and the voltage control that are necessary for a detailed and quantitative analysis of sodium channel function. Planar bilayers are well suited for this purpose. Recently, Krueger *et al.* (16) incorporated rat brain membranes containing sodium channels into planar bilayers formed from phospholipids dissolved in *n*-decane. Channel activation by BTX allowed them to record 30-pS sodium channels that were blocked by nanomolar concentrations of STX in a voltage-dependent manner. We used an experimental approach similar to that of Krueger *et al.* (16) to incorporate purified reconstituted sodium channels into planar lipid bilayers and to characterize the properties of the channel under voltage clamp conditions. Here, we show that purified sodium channels from rat brain—which consist of three polypeptide subunits: α ($M_r \approx 260{,}000$), $\beta 1$ ($M_r \approx 39{,}000$), and $\beta 2$ ($M_r \approx 37{,}000$) (5)—exhibit the voltage dependence, neurotoxin sensitivity, and ionic selectivity that are characteristic of native sodium channels. A preliminary account of this research appeared elsewhere (17).

MATERIALS AND METHODS

Materials. Phosphatidylethanolamine (PtdEtn) and phosphatidylcholine (PtdCho) from bovine brain were obtained from Sigma. Synthetic 1-palmitoyl-2-oleoyl PtdEtn and PtdCho were obtained from Avanti Polar Lipids. Porous polystyrene beads (Bio-Beads SM2) were from Bio-Rad. BTX was the generous gift of J. W. Daly (Laboratory of Bioorganic Chemistry, National Institute of Arthritis, Diabetes, and Digestive and Kidney Diseases, National Institutes of Health).

Sodium Channel Purification and Reconstitution in Lipid Vesicles. Rat brain sodium channels were purified as described by Hartshorne and Catterall (5) with the modifications described in Tamkun *et al.* (9) to a specific activity of 2000 pmol of STX binding sites per mg of protein. The purified sodium channels were reconstituted into 65% PtdCho/35% PtdEtn (bovine brain) lipid vesicles by using Bio-Beads SM2 to absorb the detergent (8, 18). The vesicle suspension contained 5 pmol of active STX binding sites per ml and 17 μg of protein per ml. Fifteen-microliter aliquots of the preparation were frozen in liquid nitrogen and stored at −70°C until use.

Channel Incorporation into Lipid Bilayers. The fusion technique was used to incorporate reconstituted sodium channel proteoliposomes into planar lipid bilayers (16, 19). Black lipid membranes were formed and their electrical properties were studied as described by Mueller and Rudin (20). Membranes were spread from a solution of 40 mg of 1-palmitoyl-2-oleoyl PtdEtn per ml and 10 mg of 1-palmitoyl-2-oleoyl PtdCho per ml in *n*-decane over a 220-μm diameter aperture in a 25-μm-thick Teflon septum that separated two 450-μl Teflon chambers. Only bilayers with specific capacitances between 0.26 and 0.34 $\mu F/cm^2$ and resistances >300 GΩ

The publication costs of this article were defrayed in part by page charge payment. This article must therefore be hereby marked "*advertisement*" in accordance with 18 U.S.C. §1734 solely to indicate this fact.

Abbreviations: BTX, batrachotoxin; TTX, tetrodotoxin; γ, single channel conductance; V, applied voltage; V_{50}, voltage at which the channel is open 50% of the time; PtdCho, phosphatidylcholine; PtdEtn, phosphatidylethanolamine; STX, saxitoxin; q, apparent gating charge.

‡To whom reprint requests should be addressed.

were used. The *cis* chamber contained 0.5 M NaCl in medium A (10 mM Hepes/Na^+, pH 7.4/0.15 mM $CaCl_2$/0.1 mM $MgCl_2$/0.05 mM EGTA). The *trans* chamber contained 0.2–0.4 M NaCl in medium A and 1 μM BTX. To the *cis* chamber, 1–5 μl of reconstituted sodium channel proteoliposomes were added and the solution was stirred for 3 min at an applied voltage (V) of 70 mV. The current through the bilayer was then examined for 1 min at V = −70 mV and V = 70 mV to determine if any sodium channels had been incorporated. If not, the bilayer capacitance was rechecked and the stirring step repeated until one or more channels were seen. Sodium channels were routinely detected within 15–30 min. Channel incorporation was stopped either by adding 4 M NaCl to the *trans* chamber to yield a final concentration of 0.5 M NaCl or by perfusing the *cis* chamber with 0.5 M NaCl medium A. All experiments were performed at 21°C ± 2°C.

Electrical Recording. A List Medical Electronics EPC-7 amplifier in voltage clamp mode was used to amplify the current and to control the voltage across the bilayer. Ag/AgCl pellet electrodes were used. The *trans* electrode was set to a command voltage relative to the *cis* electrode, which was held at virtual ground. The EPC-7 output was filtered at 3 KHz and recorded on a RACAL 4DS FM tape recorder at 19 cm/s. The tape-recorded signal was played back at the same tape speed, filtered as indicated on an 8-pole Bessel low-pass filter (Frequency Devices), and displayed on a Gould 2200 S chart recorder to obtain all of the current records shown except Fig. 1*A*.

To correct for electrode offset potentials, the reversal potential for current through the sodium channel was determined and subtracted from the Nernst potential for Na^+ under the experimental conditions. This correction factor (typically ≤2 mV) was added to the command voltage to calculate the absolute voltage applied across the bilayer.

Voltage Convention. The electrode voltage was $V_{trans} - V_{cis}$. Sodium channels incorporated into the bilayer with their normally extracellular side facing the *trans* chamber sense a voltage of opposite polarity than the *cis*-facing channels. To avoid this ambiguity, the electrophysiological convention ($V = V_{in} - V_{out}$) is used throughout this report except where "electrode voltage" is specifically indicated. The "out" side of a sodium channel can be determined either from the sidedness of the TTX block of the channel (15) or from the polarity of the hyperpolarizing electrode potential that closes the channel.

RESULTS

Channel Opening Is Voltage Dependent. The currents flowing through individual sodium channels activated by 1 μM BTX and recorded at the indicated voltages are shown in Fig. 1*A*. At −110 mV, the channel is closed most of the time with a few brief openings. At more positive potentials, the channel spends an increasing fraction of time open. At −50 mV, and more positive potentials, only occasional closures interrupt long open stretches. This effect of V on the probability of the channel being open is clearly illustrated in Fig. 1*B*, in which current histograms are shown. Two distinct Gaussian distributions are evident at each V, corresponding to the current levels of the closed and open states of the sodium channel. The area under each Gaussian is proportional to the residence time in each state. The percentage of time the channel is open at any given voltage was determined by integration and the results are plotted in Fig. 1*C*. Channel opening is favored by depolarization and is strongly voltage dependent. The voltage at which the channel is open 50% of the time (V_{50}) is −82 mV in this experiment. Depolarization increases the time spent open to a maximum of 95% at V = −60 mV. The mean maximal open percentage from four separate channels is 96.8% ± 0.8% (SEM).

The relationship between percent open time and V was transformed, as described by French *et al.* (22), into a linear function whose slope is proportional to the apparent gating charge of the channel. The purified sodium channel has an apparent gating charge of 3.8 ± 0.3 (SEM, n = 5) electronic charges per channel.

V_{50} varied considerably from channel to channel, ranging from −130 mV to −64 mV, with a mean of −91 mV ± 17 mV (SD, n = 22). The variability of V_{50} was not due to variable electrode offset potentials (see *Materials and Methods*). The curves of voltage dependence of channel opening are essentially parallel to the curve shown in Fig. 1*C* but shifted along

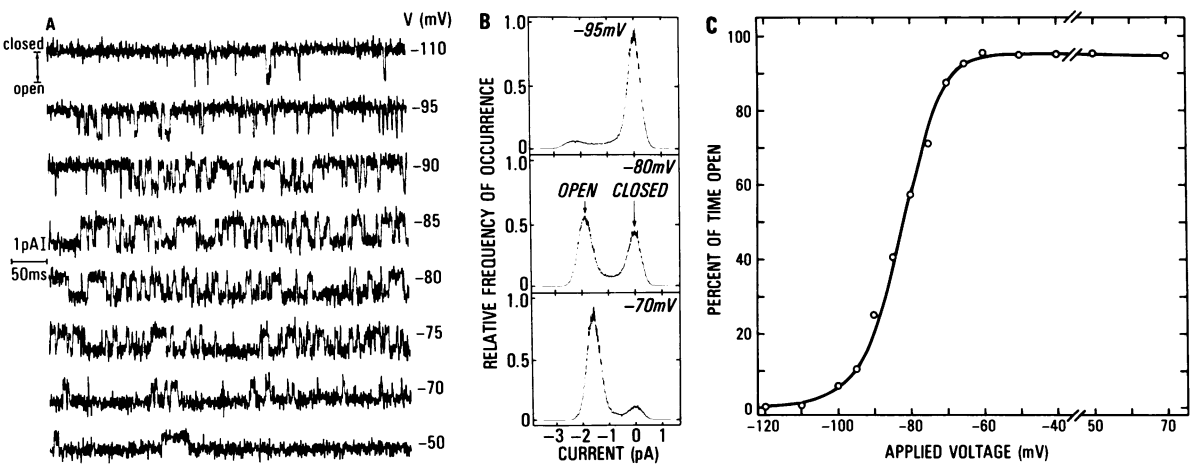

FIG. 1. Voltage dependence of sodium channel opening. The current through a single purified sodium channel bathed in 0.5 M NaCl medium A *cis* and 0.35 M NaCl medium A/1 μM BTX *trans* was recorded under voltage clamp conditions while the voltage was increased from −130 mV in steps lasting 30 s. *(A)* Representative current records at the indicated voltages were filtered at 800 Hz, digitized at a 500-μs sampling interval, and plotted by computer (21) with lines connecting the data points. *(B)* Single sodium channel current histograms at −95 mV, −80 mV, and −70 mV. At each voltage, sections of the current record 25 s long were filtered at 300 Hz, digitized at a 100-μs sampling interval, and analyzed by a computer program that plotted relative time spent at each current level. Two Gaussian distributions corresponding to the open (left peak) and closed state (right peak) of the channel are seen at each V. The relative areas under the closed and open curves reflect the probability of each state at the indicated voltage. *(C)* Voltage dependence of channel opening. The percentage of time the channel is open, computed by measuring the area under the peaks in current histograms, is plotted as a function of the V. The curve was fit to the data points by eye.

the voltage axis to the appropriate V_{50}. Thus, the variability of V_{50} does not result from the sodium channels sensing only a fraction of the applied voltage.

BTX Is Required to Detect Sodium Channels. In the presence of 1 μM BTX sodium channels show voltage-dependent activation and do not inactivate (Fig. 1). To determine if this activity is BTX dependent, experiments were done to see if channel activity would be expressed under similar conditions in the absence of BTX. In control experiments using the incorporation procedure described in *Materials and Methods* with 0.5 M NaCl medium A *cis* and 0.2 M NaCl medium A/1 μM BTX *trans*, 15 sodium channels were recorded in 8 different bilayers observed for a total of 205 min. Under identical conditions, but in the absence of BTX, no channels were detected in 8 different bilayers observed for a total of 330 min. The probability that random fluctuations in channel incorporation account for the lack of observable channels is $<10^{-4}$. Therefore, it is likely that sodium channels were incorporated into the bilayer in the absence of BTX but that BTX, by eliminating inactivation, allowed their detection under constant V conditions. At present, technical problems associated with the large capacitance of the planar lipid bilayer make it unfeasible to determine if purified sodium channels undergo purely voltage-dependent activation and inactivation in the absence of BTX.

Sodium Channels Are Blocked by TTX. The specificity of sodium channel block by TTX makes it a critical test to establish if an ionic current is flowing through a sodium channel. Fig. 2 illustrates that the ionic current through purified sodium channels is blocked by TTX, that TTX is effective only on the normally extracellular-facing side of the sodium channel, and that the TTX block is reversible. The initial current record in Fig. 2*A* shows 4 open channels. Prior examination of the voltage dependence of channel closing revealed that 3 of the channels were closed at an electrode voltage of −140 mV and 1 of the channels was closed at an electrode voltage of +140 mV. This indicates that 3 of the channels are oriented with their "extracellular" side facing the *cis* chamber and that the fourth channel is oppositely oriented. Addition of TTX to the *trans* chamber (Fig. 2*A*) quickly blocks the 1 *trans*-facing channel but has no effect on the 3 *cis*-facing channels, as expected from the extracellular orientation of the TTX binding site and the fact that TTX is membrane impermeant (15). Fig. 2*B* shows that addition of TTX to the *cis* chamber blocks the 3 *cis*-facing channels. The initial current tracing in Fig. 2*C*, on a time scale that is slower by a factor of 10, shows that the channels remain blocked as long as TTX is present. Following perfusion of the *cis* chamber to remove TTX, 3 open channels reappear, demonstrating that TTX block is reversible. The TTX sensitivity displayed by the channels convincingly demonstrates that they are indeed sodium channels.

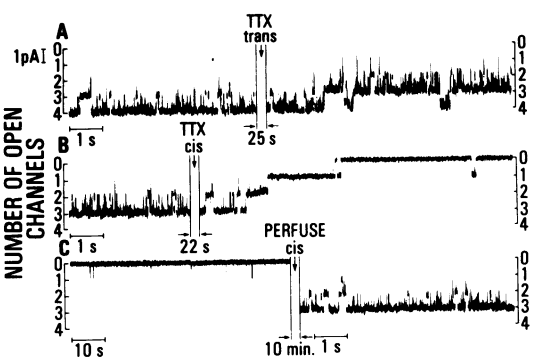

FIG. 2. TTX block of sodium channels. The bilayer contained 1 *trans*-facing and 3 *cis*-facing sodium channels in symmetric 0.5 M NaCl medium A with 1 μM BTX *trans*. To prevent incorporation of other sodium channels, the *cis* chamber was perfused with 0.5 M NaCl medium A to remove the proteoliposomes. V was −50 mV for the *cis*-facing channels and +50 mV for the *trans*-facing channel. The records were filtered at 500 Hz. *(A)* Orientation dependence of TTX block. The initial current record shows 4 open channels interrupted by occasional brief closures. At the arrow, 40 μM TTX (final concentration) was added to the *trans* chamber. The 1 *trans*-facing sodium channel is soon blocked and remains blocked during the 3 min separating the record in *A* from that in *B*, while the 3 *cis*-facing channels are unaffected. *(B)* Addition of 2 μM TTX to the *cis* chamber promptly reduces the membrane current in three discrete steps to the value it was before channels were incorporated. *(C)* Reversibility of TTX block. In the presence of 2 μM TTX, the channels remain blocked with occasional brief openings. Upon removal of TTX by perfusion of the *cis* chamber with 0.5 M NaCl medium A (exchange of 14 volumes with stirring) the membrane current returns to the pre-TTX value. The *trans*-facing channel remains blocked. Note the change in time calibration before and after perfusion.

TTX Block of Sodium Channels Is Voltage Dependent. STX and TTX block of native sodium channels in planar lipid bilayers is voltage dependent (22, 23). TTX block of purified sodium channels exhibits a similar voltage dependence. Fig. 3*A* shows the effect of 250 nM TTX *cis* on 4 *cis*-facing sodium channels at 70 mV and −50 mV. At these voltages in the

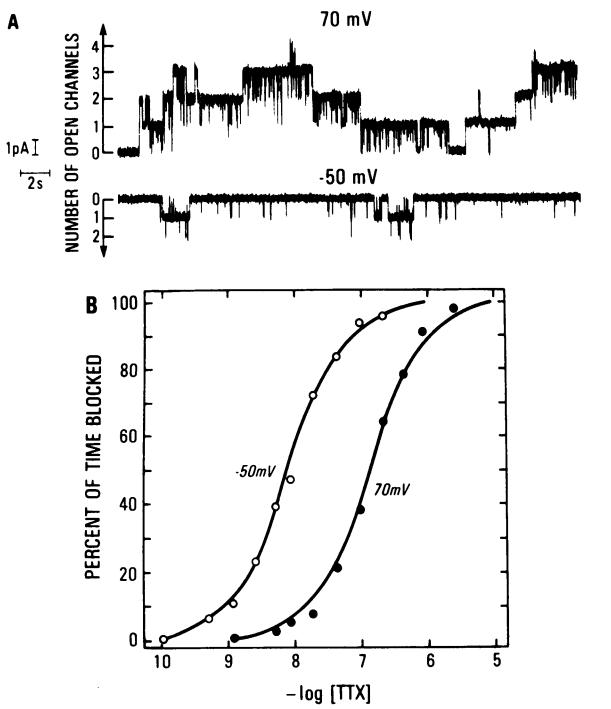

FIG. 3. Concentration and voltage dependence of the TTX block of sodium channels. *(A)* Current records at 70 mV (upper trace) and −50 mV (lower trace) from a membrane containing 4 *cis*-facing BTX-activated sodium channels in symmetric 0.5 M NaCl medium A following the addition of 250 nM TTX to the *cis* chamber. The step-like changes in current of long durations are due to TTX block and unblock of the *cis*-facing channels. Several *trans*-facing channels are in this bilayer but they were blocked by 40 μM TTX *trans*. The records were filtered at 90 Hz. *(B)* The concentration dependence of TTX block of purified sodium channels at −50 mV (○) and 70 mV (●). Current records from the bilayer described in *A* were examined to determine the percentage of time the channels were blocked as a function of the TTX concentration *cis*. Prior examination of the current records at the two voltages in the absence of TTX *cis* indicated that closures >1 s were rare. Therefore, only channel closures lasting >1 s were attributed to TTX block. To insure that representative samples of data were examined, 45-min records were analyzed for each TTX concentration < 4 nM; 30-min records were analyzed for 4 nM < TTX concentration < 20 nM; and 10-min records were analyzed for TTX concentration > 20 nM. The curves were drawn by plotting (100 [TTX])/(K_i + [TTX]) vs. −log [TTX] for K_i = 8.3 nM at −50 mV and K_i = 135 nM at 70 mV.

absence of TTX, the channels were open >95% of the time. A comparison of the two records shows clearly that the TTX block of sodium channels is antagonized by depolarization. This result is shown in quantitative detail in Fig. 3*B*, in which the concentration dependence of the TTX-induced sodium channel block at −50 mV and 70 mV is displayed. At −50 mV, the K_i for the TTX block is 8.3 nM, whereas at 70 mV it increases to 135 nM. The voltage dependence of the change in K_i corresponds to an *e*-fold increase in K_i for a 43-mV depolarization.

Sodium Channels Are Sodium Selective. A purified sodium channel that is functionally intact should have a high permeability to Na^+ relative to other monovalent cations. Fig. 4*A* shows single channel currents recorded at 100 mV from BTX-activated sodium channels in symmetric 0.5 M solutions of NaCl, KCl, and RbCl. The amplitudes of the single channel currents (Na^+ = 2.5 pA, K^+ = 0.32 pA, and Rb^+ = 0.11 pA) reflect the relative permeability of the cations. The small current in Rb^+ is difficult to resolve from the noise unless the bilayer is held at a positive voltage where the channel is open >95% of the time and 200 nM TTX is present to create long closed stretches. The records in Fig. 4*A* are then filtered at 50 Hz to resolve the open and TTX-blocked states of the channel.

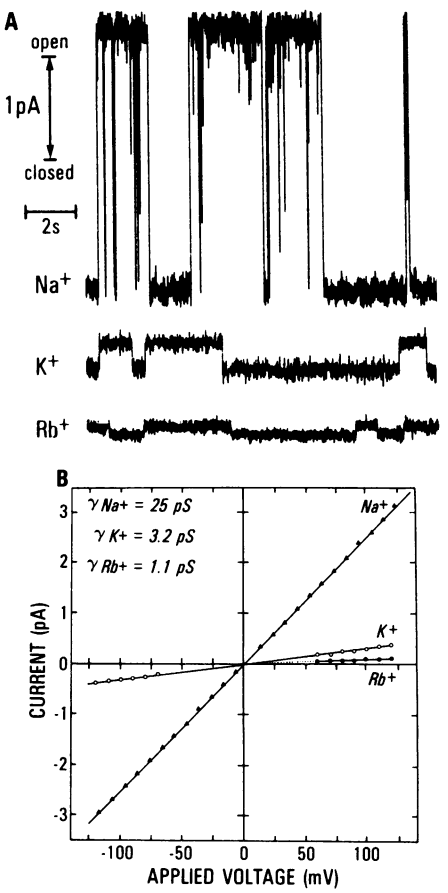

FIG. 4. Ionic selectivity of the BTX-activated sodium channels. *(A)* Single sodium channel currents in different monovalent cations. Single channel currents through a *cis*-facing sodium channel in symmetric 0.5 M NaCl medium B (10 mM Hepes/Tris, pH 7.4/0.15 mM $CaCl_2$/0.1 mM $MgCl_2$/0.05 mM EGTA) containing 200 nM TTX *cis* (upper record). The single channel currents in symmetric 0.5 M KCl medium B (middle record) and 0.5 M RbCl medium B (lower record) were recorded after replacing NaCl from both chambers with either KCl or RbCl by perfusion (7 volumes with stirring) and adding 200 nM TTX *cis*. After the current–voltage characteristics were measured, 40 μM TTX was added to the *cis* chamber, which blocked the currents completely. The records were obtained at 100 mV and were filtered at 50 Hz. *(B)* Current–voltage relationship of single sodium channels in 0.5 M symmetric solutions of NaCl (▲), KCL (○), and RbCl (●) in medium B. The continuous lines are the least square fits to the data points: the slope conductances were γ_{Na^+} = 25 pS, γ_{K^+} = 3.2 pS, and γ_{Rb^+} = 1.1 pS. The uncorrected zero-current membrane potentials were 1.4 mV and 1.5 mV for Na^+ and K^+, respectively.

Fig. 4*B* shows the single channel current–voltage curves for BTX-activated sodium channels in 0.5 M symmetric solutions of NaCl, KCl, and RbCl. For the experimental reasons just given, only the positive branch of the current–voltage relationship in Rb^+ is shown. In each case, the current–voltage relationship is linear over the voltage range studied with a zero current membrane potential near zero mV. The single channel conductance, γ, of the sodium channel for each cation calculated from the slopes of the lines in Fig. 4*A* is displayed in the *Inset*. The average values for all experiments are γ_{Na^+} = 25.2 pS ± 0.5 pS (SEM, n = 10), γ_{K^+} = 3.5 pS ± 0.2 pS (SEM, n = 3), and γ_{Rb^+} = 1.2 pS ± 0.1 pS (SEM, n = 3). The permeabilities of the cations relative to Na^+ are P_{Na^+} = 1, P_{K^+} = 0.14 ± 0.02, and P_{Rb^+} = 0.05 ± 0.01, demonstrating that the purified sodium channel retains its ionic selectivity.

DISCUSSION

Previous work demonstrated that the purified "saxitoxin receptor" from rat brain consists of three subunits: α (M_r = 260,000), β1 (M_r = 39,000), and β2 (M_r = 37,000) (5). Reconstitution experiments showing that the purified protein mediates a veratridine-stimulated and TTX-inhibitable $^{22}Na^+$ flux justified the application of the term sodium channel to the purified protein (8, 9). In this study, purified sodium channels incorporated into planar lipid bilayers were examined under voltage clamp conditions in the presence of BTX to determine the voltage dependence of activation, the concentration and voltage dependence of TTX block, the single channel conductance, and the ionic selectivity. The functional properties of purified reconstituted sodium channels are in remarkable agreement with those exhibited by native rat brain sodium channels, as summarized in Table 1.

Our results differ in several respects from those reported by Hanke *et al.*, who studied sodium channels evidently devoid of β_1 and β_2 subunits (26). It will be interesting to compare in detail the differences between their preparation and ours.

A few observations deserve particular comment. The voltage dependence of sodium channel activation in BTX is characterized by two parameters, V_{50} and q. Table 1 shows good agreement between purified and native sodium chan-

Table 1. Comparison of functional properties of purified and native sodium channels from rat brain

Property	Purified	Native
V_{50} for channel opening	−91 mV	−93 mV (22)
Apparent gating charge (q)	3.8	4–6 (22)
BTX removes inactivation	Yes	Yes (16)
BTX $K_{0.5}$	2 μM (9)	0.5 μM (24)
Veratridine $K_{0.5}$	30 μM (9)	14 μM (24)
TTX/STX block is orientation dependent	Yes (8)	Yes (16)
TTX K_i at V = −50 mV	8.3 nM	7–16 nM*
mV/*e*-fold shift in K_i (TTX)	43 mV	35–41 mV*
Voltage-dependent Lqtx† binding	Yes (18)	Yes (25)
γ (0.5 M NaCl)	25 pS	30 pS (16)
Permeability relative to Na^+		
P_{K^+}	0.14	0.07 (16)
P_{Rb^+}	0.05	ND

References are given in parentheses. ND, not determined.
*R. J. French and B. K. Krueger, personal communication.
†Lqtx = scorpion toxin (*Leiurus quinquestriatus*).

nels in planar bilayers for these parameters. Similar results were found in frog node of Ranvier (V_{50} = −90 mV ± 10 mV, q = 3.5) (12) and neuroblastoma cell line NG108-15 (V_{50} = −85 mV, q = 4–5) (13, 27). Therefore, both the voltage-sensing and the gating apparatus are present and functional in the purified sodium channel.

The V_{50} for purified channels varied considerably while q was essentially constant. V_{50} also varies considerably in native sodium channels, ranging from −105 mV to −75 mV in dog brain sodium channels (28). In native rat brain sodium channels, the variability of V_{50} (SD = 9 mV, n = 3) is apparently less (22). The reason for the variability of V_{50} is unclear, but it may reflect inherent differences in voltage sensitivity of sodium channels, which may arise from variations in fixed charges on or near the channel protein.

TTX block of purified reconstituted sodium channels is *(i)* reversible, *(ii)* dependent on the orientation of the channel, and *(iii)* voltage dependent, in agreement with findings in native rat brain sodium channels (Table 1). The latter characteristic appears to reflect a voltage-dependent conformational change of the channel protein rather than the migration of the charged toxin in the direction of the applied electric field (23). These results unambiguously identify the ion channel investigated in this study as the sodium channel and demonstrate that the TTX binding site is present and functional in purified reconstituted sodium channels.

The purified sodium channel activated by BTX has one well-defined open conductance state of 25 pS. This is lower than the single channel conductance of 30 pS reported for native rat brain sodium channels incorporated into 30% phosphatidylserine/70% PtdEtn bilayers in the same ionic medium (16, 22). The small difference in γ may arise from the differences in lipid environments. The γ of the K^+ channel from sarcoplasmic reticulum, for example, is higher in negatively charged phosphatidylserine/PtdEtn membranes than in neutral PtdCho/PtdEtn membranes (29).

The purified sodium channel is more permeable to Na^+ than K^+ or Rb^+. The permeability ratios for purified sodium channels given in Table 1 are direct measurements of the single channel conductance ratios in symmetric 0.5 M solutions of chloride salts of the cations. The relative permeability of K^+ to Na^+ through native sodium channels, estimated from reversal potential measurements, agrees qualitatively with that determined from purified sodium channels. The quantitative difference between the two values may arise from the known dependence of permeabilities calculated from reversal potentials on the ionic composition of the bathing medium (30). Values for the permeability ratios agree well with those found for BTX-activated sodium channels in neuroblastoma N18 cells (P_{Na^+} = 1, P_{K^+} = 0.17, P_{Rb^+} = 0.08) (31) and for BTX-activated sodium channels purified from rat muscle (P_{Na^+} = 1, P_{K^+} = 0.14, P_{Rb^+} = 0.02) (32). Thus, the "ion selectivity filter" is present and functional in purified sodium channels.

The results listed in Table 1 show that the purified sodium channel protein contains a functional veratridine/BTX binding site, STX/TTX binding site, scorpion toxin binding site, voltage-sensing mechanism, ion-conducting pore, and ion selectivity filter. Therefore, all of these elements of the sodium channel and almost certainly the entire structure of the rat brain sodium channel are contained within the α, $\beta 1$, and $\beta 2$ subunits of the purified protein.

Voltage-dependent activation and inactivation in the absence of BTX remain to be observed. Overcoming the technical problems associated with this task will be our next objective. Beyond that, the functional role of each of the three subunits remains to be established. Because the planar lipid bilayer system provides an accessible, well-defined environment for biochemical modification of the sodium channel protein under conditions in which the functional activity of a single sodium channel molecule can be simultaneously monitored, it will be a powerful tool in determining the relationship between sodium channel structure and function.

Note Added in Proof. While this manuscript was in press, Rosenberg *et al.* (33) reported the voltage-dependent activation of reconstituted sodium channels purified from electric eel.

We are indebted to Larry Weiss for his helpful suggestions and to Tony Lee for his assistance with the computer programs. This research was supported by grants from the National Institutes of Health (EY-02084 to M.M. and N.S. 15751 to W.A.C.) and The Department of the Army Medical Research (17-82-C221 to M.M.). R.P.H. is a Postdoctoral Fellow of the National Multiple Sclerosis Society and B.U.K. is a fellow of the Education Abroad Program.

1. Hille, B. (1978) *Biophys. J.* **22,** 283–294.
2. Agnew, W. S., Levinson, S. R., Brabson, J. S. & Raftery, M. A. (1978) *Proc. Natl. Acad. Sci. USA* **75,** 2606–2610.
3. Miller, J. A., Agnew, W. S. & Levinson, S. R. (1983) *Biochemistry* **22,** 462–470.
4. Hartshorne, R. P. & Catterall, W. A. (1981) *Proc. Natl. Acad. Sci. USA* **78,** 4620–4624.
5. Hartshorne, R. P. & Catterall, W. A. (1984) *J. Biol. Chem.* **259,** 1667–1675.
6. Barchi, R. L., Cohen, S. A. & Murphy, L. E. (1980) *Proc. Natl. Acad. Sci. USA* **77,** 1306–1310.
7. Barchi, R. L. (1983) *J. Neurochem.* **40,** 1377–1385.
8. Talvenheimo, J. A., Tamkun, M. M. & Catterall, W. A. (1982) *J. Biol. Chem.* **257,** 11868–11871.
9. Tamkun, M. M., Talvenheimo, J. A. & Catterall, W. A. (1984) *J. Biol. Chem.* **259,** 1676–1688.
10. Weigele, J. B. & Barchi, R. L. (1982) *Proc. Natl. Acad. Sci. USA* **79,** 3651–3655.
11. Rosenberg, R. L., Tomiko, S. A. & Agnew, W. S. (1984) *Proc. Natl. Acad. Sci. USA* **81,** 1239–1243.
12. Khodorov, B. I. & Revenko, S. V. (1979) *Neuroscience* **4,** 1315–1330.
13. Huang, L. M., Moran, N. & Ehrenstein, G. (1982) *Proc. Natl. Acad. Sci. USA* **79,** 2082–2085.
14. Catterall, W. A. (1980) *Annu. Rev. Pharmacol. Toxicol.* **20,** 15–43.
15. Narahashi, T., Anderson, N. C. & Moore, J. W. (1966) *Science* **153,** 765–767.
16. Krueger, B. K., Worley, J. F., III, & French, R. J. (1983) *Nature (London)* **303,** 172–175.
17. Hartshorne, R. P., Keller, B., Talvenheimo, J. A., Catterall, W. A. & Montal, M. (1984) *Soc. Neurosci.*, 864, abstr. 10.
18. Feller, D. J., Talvenheimo, J. A. & Catterall, W. A. (1984) *Soc. Neurosci.*, 863, abstr. 10.
19. Miller, C. & Racker, E. (1976) *J. Membr. Biol.* **30,** 283–300.
20. Mueller, P. & Rudin, D. O. (1969) in *Laboratory Techniques in Membrane Biophysics*, eds. Passow, A. & Stampfli, R. (Springer, Heidelberg), pp. 141–156.
21. Labarca, P., Lindstrom, J. & Montal, M. (1984) *J. Gen. Physiol.* **83,** 473–496.
22. French, R. J., Worley, J. F., III, & Krueger, B. K. (1984) *Biophys. J.* **45,** 301–310.
23. Moczydlowski, E., Hall, S., Garber, S., Strichartz, G. & Miller, C. (1984) *J. Gen. Physiol.* **84,** 687–704.
24. Tamkun, M. M. & Catterall, W. A. (1981) *Mol. Pharmacol.* **19,** 78–86.
25. Ray, R., Morrow, C. S. & Catterall, W. A. (1978) *J. Biol. Chem.* **253,** 7307–7313.
26. Hanke, W., Boheim, G., Barhanin, J., Pauron, D. & Lazdunski, M. (1984) *EMBO J.* **3,** 509–515.
27. Huang, L. M., Moran, N. & Ehrenstein, G. (1984) *Biophys. J.* **45,** 313–322.
28. Weiss, L. B., Green, W. N. & Andersen, O. S. (1984) *Biophys. J.* **45,** 67 (abstr.).
29. Bell, J. E. & Miller, C. (1984) *Biophys. J.* **45,** 279–287.
30. Cahalan, M. & Begenisich, T. (1976) *J. Gen. Physiol.* **68,** 111–125.
31. Huang, L. M., Catterall, W. A. & Ehrenstein, G. (1979) *J. Gen. Physiol.* **73,** 839–854.
32. Tanaka, J. C., Eccleston, J. F. & Barchi, R. L. (1983) *J. Biol. Chem.* **258,** 7519–7526.
33. Rosenberg, R. L., Tomiko, S. A. & Agnew, W. S. (1984) *Proc. Natl. Acad. Sci. USA* **81,** 5594–5598.